Materials Science-Poland, Vol. 28, No. 1, 2010

First principles study on the improved dehydrogenating properties of MgH_2 systems with metal fluorides

D.W. ZHOU[1*], J.S. LIU[2], S.H. XU[2], G.Y. CHEN[1]

[1]State Key Laboratory of Advanced Design and Manufacturing for Vehicle Body,
Hunan University, Changsha 410082, P.R. China

[2]School of Materials Science and Engineering, Hunan University, Changsha 410082, P.R. China

Energies and electronic structures of MgH_2 systems were determined from the first principles calculations to explain the improving of their dehydrogenating properties by addition of metal fluorides as catalysts. These calculations show that a Mg vacancy can improve the thermodynamics of MgH_2 systems and Mg atom replaced for Fe, Ti, Zr, V, Ni, Nb, Cr, Cu is energetically more favourable than formation of Mg vacancies at lower temperatures. Calculations of density of states (DOS) provide a particularly good explanation for a close agreement between the experimental results and theoretical predictions for improvements to the dehydrogenation kinetics of MgH_2 systems for NiF_2, NbF_5, ZrF_4 used as the catalysts.

Keywords: *MgH_2; density functional theory; dehydrogenating properties*

1. Introduction

Magnesium hydride (MgH_2) is a promising material for hydrogen storage applications, as it has high gravimetric (7.6 wt. %) and volumetric (110 $kg\cdot m^{-3}$) densities. Moreover, its reversibility and cycle performance are quite good compared with other binary and complex hydrides of I and II groups. However, magnesium hydride has a high dissociation temperature and relatively high thermal stability, resulting in its slow re-hydrogenation and de-hydrogenation kinetics. This therefore limits its practical application as a good hydrogen storage material.

The kinetics of sluggish hydrogenation was found to be significantly improved by fabricating fine nanocrystalline Mg particles, by the mechanical alloying method [1, 2]. Although a high desorption temperature still remains a problem to be solved, the mechanical alloying of MgH_2 and 3d transition metals (Ni, Co, Mn, Cu, Ti, Fe, V, etc. [3, 4]), 3d non-transition metals (Ge, Nb, etc. [3, 5]), intermetallic compounds

---

[*] Corresponding author, e-mail: ZDWe_mail@yahoo.com.cn

($LaNi_5$, FeTi, $ZrFe_{1.4}Cr_{0.6}$, etc. [6–8]), metal oxides (Nb_2O_5, Fe_3O_4, etc [9]), effectively improve the hydriding and dehydrogenating kinetics of MgH_2 at high temperatures. Recently, Jin et al. [10] systematically investigated various metal fluorides (such as FeF_2, NiF_2, TiF_3, NbF_5, CuF_2, VF_4, ZrF_4, CrF_2, etc.) and their catalytic effect on the dehydrogenation and hydrogenation characteristics of MgH_2 powder. They have found that metal fluorides are the most suitable catalysts for the re/dehydrogenation of MgH_2. They ranked the following in order of increasing catalytic performance: CuF_2, CrF_2, ZrF_4, FeF_2, NbF_5, VF_4, TiF_3, NiF_2.

Some considerable experimental and theoretical investigations have been performed on the improved dehydrogenating properties of MgH_2 systems. Based on X-ray scattering measurements and phase structural change analysis, Pelletier et al. [9] suggested that the improved kinetics in Nb doped MgH_2 is due to the formation of niobium hydride, which leads to the nucleation of the α-Mg at the β-NbH/β-MgH_2 interface. Song et al. [11], Shang et al. [3] and Li et al. [12] calculated the total energy and electronic structure of MgH_2 solid solution in order to study the mechanism of the improvement to the dehydrogenating properties of MgH_2 systems with metal elements (Al, Ti, Fe, Ni, Cu, Nb, etc.) and metal oxides (Nb_2O_5, etc.). In the examined group, the energy and electronic structure of the adsorption of H_2 on a clean, vacancy defective Mg(0001) surface and iron alloying MgH_2 were calculated by using the first principles plane-wave pseudopotential method. The improved properties of MgH_2 systems are also analyzed with respect to the milling process and iron addition [13]. Moreover, based on the energy calculations of $VH_{0.81}$ phase, and the design and exploitation of a VH/MgH_2 interface model, the vanadium alloying effects on the dehydrogenating properties [14] and diffusion and adsorption of H atoms [15] of MgH_2–V system have been investigated [15].

Jin et al. [10] investigated the catalytic performance of different metal fluorides on MgH_2, and they concluded that NiF_2 performed best. Nevertheless, it is still not clear how these chemically different additives promote the dehydrogenation and hydrogenation reactions of MgH_2. As for as the improved dehydrogenating properties of MgH_2 systems with NiF_2 are concerned, MgF_2 and Mg_2NiH_4 are detected in the reaction products during high-energy milling process, as reported by Jin et al. [10]. It is believed that MgF_2 and Mg_2NiH_4 form by the following displacement reaction: $NiF_2 + 3MgH_2 = MgF_2 + Mg_2NiH_4$. One could assume that MgF_2 formation is caused by the Mg atom of MgH_2 and the F atom of NiF_3, thus some Mg vacancies which remain in the sample, may affect desorption of hydrogen. If an Ni atom of NiF_3 replaces a Mg atom of MgH_2, it forms $(Mg,Ni)H_x$ solid solution, which can be changed into Mg_2NiH_4 hydrides, thus the electronic structure of the considered systems is locally changed. Hence, both Ni substitution and Mg vacancies have an effect on the dehydrogenating properties of MgH_2 systems.

Based on the above analysis, in the present work, the bonding distance change for Mg–H and Ni–H, the energy to remove H atoms and electronic structure of MgH_2 systems have been calculated by using the Dmol 4.1 program based on the density functional theory. The improved properties of MgH_2 systems with metal fluorides (NiF_2, TiF_3, VF_4, NbF_5,FeF_2, ZrF_4, etc.) have also been analyzed, some new results are expected to be of theoretical guidance for designing advanced magnesium-based hydrogen storage materials.

2. Models and method of computation

The energy and electronic structure of MgH_2 systems with metal fluorides were investigated by constructing 2×2×2 supercell models consisting of 48 atoms ($Mg_{16}H_{32}$) (Fig. 1a) [12]. Here, the lattice parameters of MgH_2 with a tetragonal symmetry (*P*4/*mnm*, group No.136) are $a = 0.\ 4501$ nm and $c = 0.3010$ nm [11].

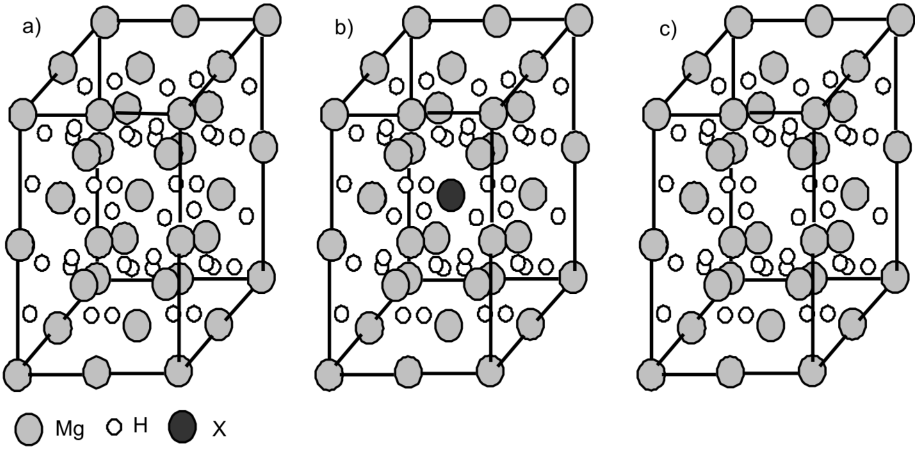

Fig. 1. Supercell model: a) $Mg_{16}H_{32}$, b) $Mg_{15}XH_{32}$ (X = Ni, Ti, V, Nb, Fe, Zr, Cr, Cu), c) $Mg_{15}H_{32}$

To simulate element substitution or a vacancy at the Mg 2*a* site (0.5, 0.5, 0.5), we considered $Mg_{15}XH_{32}$ (X = Ni, Ti, V, Nb, Fe, Zr, Cr, Cu, Fig. 1b) and $Mg_{15}H_{32}$ (Fig. 1c) supercell models, respectively. In the present work, the optimized structure, the total energy and electronic structure calculations are performed by the the DMol^3 package, which is based on density functional theory (DFT). The PWC [16] exchange correlation functional is adopted for LDA correction [17]. Sampling of the irreducible wedge of the Brillouin zone is performed with a regular Monkhorst–Pack grid of special *k*-points [18]. The positions of selected atoms in the structures are relaxed to get the final structure with minimum total energy. The convergence criteria of optimization are 1.0×10^{-5} Ha, 0.004 Ha/Å and 0.005 Å for energy, gradient and atomic displacement, respectively. To assess the accuracy of the method as well as of the computational models, a series of calculations has been performed on the bulk properties of the *hcp*-Mg and H_2 molecules correlated with the MgH_2 supercell models. In Table 1, the calculated equilibrium lattice constants *a*, *c* are listed, and *c*/*a* of *hcp*-Mg bulk, the bond length ($d_{H–H}$) of a free H_2 molecule as well as their cohesive energies (E_{tot}). The equilibrium lattice constants *a*, *c* and *c*/*a* of hcp-Mg bulk are estimated to be 0.31751 nm, 0.51504 nm and 1.6240, respectively; this is in good agreement with the experimental values [19] and other calculations [20], and the error of the *c*/*a* ratio, calculated here relative to the experimental result, is only 0.06%. The bond length of a free H_2 molecule is calculated to be 0.07490 nm, which gives a relative error of only 1.08% compared with the experimental value [21]. Meanwhile, their calculated cohesive energies (E_{tot}) are also close to the experimental data [19] and other calculated data [20]. Thus, the geometrical and electronic structures of the MgH_2 supercell models have been calculated the same conditions.

Table 1. The calculated equilibrium lattice constants *a*, *c* and *c*/*a* of *hcp*-Mg bulk, the bond length $d_{H–H}$ of a free H_2 molecule as well as their cohesive energies E_{coh}

Source	*hcp*-Mg				H_2	
	Equilibrium lattice constants			E_{coh} /(eV·atom^{-1})	Bond length/nm	E_{coh} /(eV·atom^{-1})
	a/nm	*c*/nm	*c*/*a*			
Present work	0.31751	0.51504	1.6240	1.4942	0.07490	4.5502
Experimental [19, 21]	0.321	0.521	1.62	1.51	0.0741	4.74
Ref. [20]	0.318	0.524	1.65	1.48	0.075	4.56

In our calculations of the phase stability of the MgH_2 system with a Mg vacancy under high temperature, it is relaxed through NVT molecular dynamics for 0.01 ps with a time step of 1.0 fs. The BLYP exchange-correlation functional is adopted for GGA correction. All electron Kohn–Sham wave functions are expanded in a double numerical basis with a polarized orbital (DNP).

3. Results and discussion

3.1. Effect of Ni substitution on the dehydrogenating properties of MgH_2 systems

In MgH_2 (see Fig. 2), the bonding distances with Mg at the 2*a* site (Mg(0), Fig. 2b) and its first nearest neighbour H atom (H(A), Fig. 2b) and second nearest H atom (H(B), Fig. 2b) are analyzed, as shown in Fig. 3. The results show that the distance of Mg(0)–H(A) and Mg(0)–H(B) are 0.1935 nm and 0.1955 nm, respectively. We then replace one Mg atom at the 2*a* (0.5, 0.5, 0.5) site with a Ni atom (Fig. 1b). Similarly to the case of MgH_2, the corresponding Ni–H(A) and Ni–H(B) bond lengths are shorter compared with those of Mg–H(A) and Mg–H(B), and decrease by 0.0297 nm and 0.0245 nm, respectively. When H(A) is removed, there is no observable difference in the bonding distance between the H(B) and Mg(0) atoms (Fig. 4, NO, NO1 denote MgH_2 systems with no H atom removed and one H atom removed, respectively). After Ni substitution, the distance between the Mg(0) and H(B) atom is 0.167 nm, which is also shorter compared with that (0.1710 nm) of the unchanged structure. Thus, one can visualize the Ni atom as playing the role of a magnet that continues to attract nearby H atoms as the very nearest ones are successively desorbed.

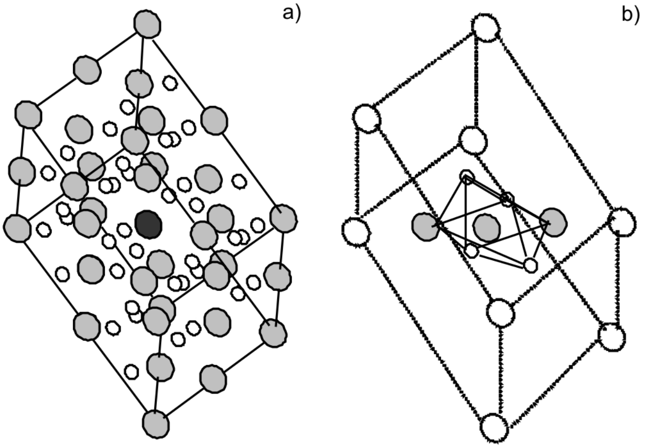

Fig. 2. Supercell model of MgH_2 (a) and supercell octahedral (b)

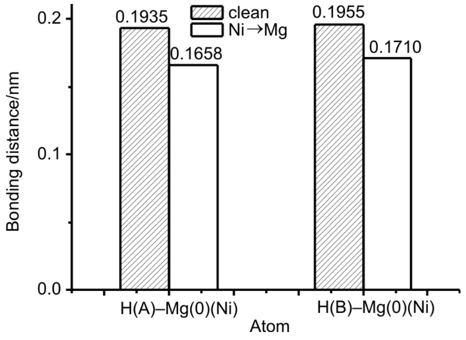

Fig. 3. The H–Mg(Ni) atom bonding distance change

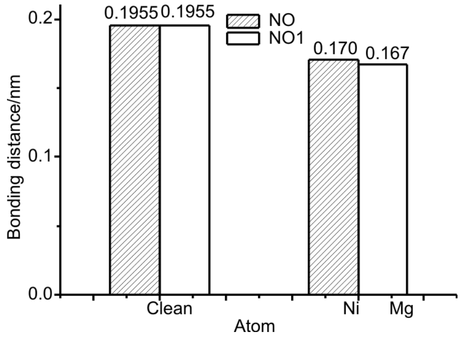

Fig. 4. The H(B–Mg(0)(Ni) atom bonding distance change

The energy costs to remove H atoms from intrinsic MgH_2 as well as the energy costs associated with Ni substitution at the Mg site are calculated by using the following equation [19]:

$$E_{\mathrm{coh}} = E(\mathrm{Mg}_{16-x}\mathrm{Ni}_x\mathrm{H}_{32-n}) - E(\mathrm{Mg}_{16-x}\mathrm{Ni}_x\mathrm{H}_{32}) + (n/2)E(\mathrm{H}_2) \tag{1}$$

The subscripts x and n refer to the number of Ni and H atoms, respectively, in the supercell that are removed, and E_{coh} refers to the cohesive energy at 0 K, defined with respect to the dissociated atoms. The calculated energies of MgH_2 systems are given in Fig. 5 (NO2 denotes MgH_2 system with two atoms removed). We find that 1.77 eV are required to remove a hydrogen atom in pure MgH_2, and 1.90 eV are required to remove two hydrogen atoms from the vicinity of the same. In contrast, in Ni doped MgH_2, the energy cost of removing one or two H atoms is 0.75 eV and 1.61 eV at 0 K, respectively, which is marginally less than that required in the case of H atom removal from pure MgH_2. This dramatic decrease in energy costs originates from structural changes following hydrogen removal from different positions, which means that Ni substitution plays an important role in the dehydrogenation properties of MgH_2 systems.

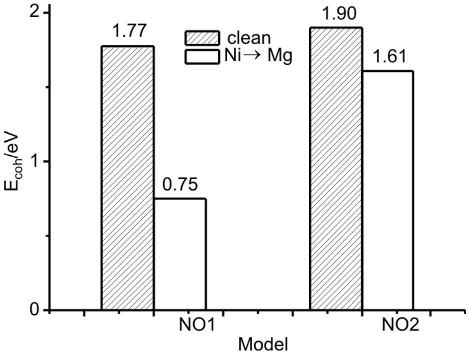

Fig. 5. The critical energy needed to remove H atoms in MgH_2 systems

3.2. Effect of Mg vacancy on the dehydrogenating properties of MgH_2 systems

Jin et al. [10] pointed out that the improved kinetics in MgH_2 systems for NiF_2 may be due to high density defects but the nature of these defects is not identified. Moreover, MgF_2 has been found to form during ball milling of MgH_2, which is also correlated to Mg vacancies. Here, we study the role of Mg vacancies on hydrogen desorption; a Mg vacancy is created from MgH_2 supercells, and the resulting changes in the H–H bonding distance are listed in Table 2.

Table 2. The differences in the H-H atom bonding distance for MgH_2 systems with/without Mg vacancy

Supercell model	Temperature/K	H(B)–H(B)/nm	H(A)–H(B)/nm	H(A)–H(A)/nm
$Mg_{15}H_{32}$	0	0.4134	0.2796	0.3766
$Mg_{15}H_{30}$	0	0.3087	0.2924	–
$Mg_{15}H_{30}$	325	0.2992	0.2789	–
$Mg_{15}H_{30}$	473	0.2960	0.2780	–
$Mg_{15}H_{30}$	673	0.2926	0.2773	–

Based on the data from the Table 2, it can be seen that the bonding distance between two H atoms in MgH_2 systems with a Mg vacancy is 0.2796 nm, longer compared with that (0.0741 nm) of hydrogen molecule. This therefore means that no hydrogen molecule formation is observed during 0 K optimization, because when two hydrogen atoms, i.e., H(A) and H(B) (Fig. 2b), are removed, the bonding distance is 0.2924 nm, meaning that no hydrogen molecule can form. To check whether there are energy barriers that cannot be overcome at 0 K during dehydrogenation, we consider temperatures of 325 K, 473 K or 673 K. The corresponding two H atoms are found to bond to each other at the distances of 0.2924 nm, 0.2780 nm and 0.2773 nm, respectively (Fig. 6). Although Mg vacancy is created, no hydrogen molecule formation is observed during optimization at 0–673 K, based on analysis of changes in the bonding distances. The H–H bonding distances at 325 K, 473 K or 673 K are all shorter than that at 0 K, lying in the trend for hydrogen molecule formation, which hints that the thermodynamics of the considered systems can be improved. This is consistent with the dynamics of hydrogen molecule formation, and suggests that the thermodynamics of the considered systems can be improved.

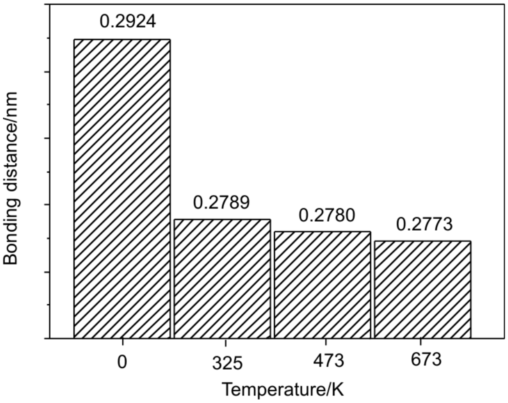

Fig. 6. The H–H atom bonding distance change at various temperatures

Further calculation is done to check whether there are benefits for the dehydrogenation of MgH_2 systems having a Mg vacancy, it is found that the energy cost of removing a hydrogen molecule from the vicinity of a Mg vacancy is –2.76 eV. The negative sign means that energy is gained if a hydrogen molecule is removed from the vicinity of a Mg vacancy and therefore the dehydrogenation process is exothermic. Based on the above analysis, a Mg vacancy also plays an important role in the dehydrogenation properties of MgH_2 systems [22].

3.3. Improved dehydrogenating properties of MgH_2 systems with NiF_2

Based on the analyses of sections 2.1 and 2.2, one can see that both Ni substitution as well as Mg vacancies both play an important role in dehydrogenation, so which of these two cases is most effective for desorbing hydrogen at lower temperatures? Clearly it is important to firstly know the energies of their formation. The formation energy of a Ni atom substituted at the Mg site is calculated using the following equation [23]:

$$H_1 = \left[E\left(\mathrm{Mg}_{15}\mathrm{NiH}_{32}\right) + E\left(\mathrm{Mg}\right)\right] - \left[E\left(\mathrm{Ni}\right) + E\left(\mathrm{Mg}_{16}\mathrm{H}_{32}\right)\right] \tag{2}$$

The formation energy of a Mg vacancy is computed from cohesive energies for the $Mg_{16}H_{32}$ and and $Mg_{15}H_{32}$ supercells, using the following equation [23]:

$$E\left(\mathrm{Mg}_{15}\mathrm{H}_{32}\right) + E\left(\mathrm{Mg}\right) - E\left(\mathrm{Mg}_{16}\mathrm{H}_{32}\right) \tag{3}$$

The calculated energy of vacancy formation is 6.51 eV; this value is higher than the one obtained by Li (3.87 eV) [12], although different methods should produce similar results. The formation energy of the Mg vacancy is much higher than the 2.12 eV needed to substitute Ni at the Mg site assuming all other conditions remain unchanged. Thus, although both Ni substitution and Mg vacancies are found to be effective in desorbing hydrogen at lower temperatures, Ni substitution is more energy efficient than the formation of Mg vacancies. If an Ni atom of NiF_2 can replace a Mg atom belonging to a MgH_2 system, the reaction $NiF_2 + 3MgH_2 = MgF_2 + Mg_2NiH_4$, occurring during the milling process, is accelerated. Thus MgH_2 with the higher stability can be changed into Mg_2NiH_4. In Sect. 2.1, regarding the removal of one first nearest neighbouring H atom, the Ni atom plays the role of a magnet that continues to attract its second nearest H atom as the nearest ones are successively desorbed, thus, it can be thought that there lies in the trend for NiH_x cluster formation, MgH_2 may be changed into $(Mg,Ni)H_x$ solid solution due to the substitution of Ni at the Mg site, while $(Mg,Ni)H_x$ solution is a likely the pathway for dehydrogenation in MgH_2 [10], and which lead to Mg_2NiH_4 formation. In the experiment undertaken by Jin et al. [10], MgF_2 and Mg_2NiH_4 were detected in the reaction products during the milling process, which is in agreement with the above analysis. Moreover, the experimental value for the formation heat of Mg_2NiH_4 is –62.7 kJ/mol H_2 [24] which is larger than that (–76.15 ± 9.2 kJ/(mol H_2) [24]) for MgH_2, which means that the H atoms of MgH_2 can be released more easily than those in Mg_2NiH_4. Hence, when a Ni atom of NiF_2 replaces a Mg atom belonging to a MgH_2 system at lower temperatures, the reaction $NiF_2 + 3MgH_2 = MgF_2 + Mg_2NiH_4$ is accelerated. Thus, MgH_2 having higher stability can be changed into Mg_2NiH_4 with lower stability. Due to formation of ternary hydride Mg_2NiH_4 with the lower stability, the dehydrogenating properties of Ni doped MgH_2 systems are improved.

3.4. Improved dehydrogenating properties of MgH_2 systems with metal fluorides

As far as the improved dehydrogenating properties of MgH_2 systems with the addition of TiF_3, VF_4, NbF_5, FeF_2, ZrF_4 are concerned, the corresponding phase of MgF_2, TiH_2, V_3H_2, NbH, Mg_2FeH_6, ZrH_2 were also detected in the reaction products during the milling process by Jin et al. [10]. It is believed that MgF_2, TiH_2, V_3H_2, NbH, Mg_2FeH_6, ZrH_2 are formed by the following displacement reactions:

$$TiF_3 + 3MgH_2 = 3MgF_2 + 2TiH_2 + H_2$$

$$3VF_4 + 6MgH_2 = 6MgF_2 + V_3H_2 + 5H2$$

$$2NbF5 + 5MgH_2 = 5MgF_2 + 2NbH + 4H_2$$

$$FeF_2 + 3MgH_2 = MgF_2 + Mg_2FeH_6$$

$$ZrF_4 + 2MgH_2 = 2MgF_2 + ZrH_2$$

Similarly, it is assumed that MgF_2 is formed by a Mg atom of MgH_2 and a F atom of TiF_3, VF_4, NbF_5, FeF_2, ZrF_4, respectively. Thus some Mg vacancies remain in the sample, while Ti, V, Nb, Fe, Zr atoms of TiF_3, VF_4, NbF_5, FeF_2, ZrF_4 replace a Mg atom of MgH_2, which will lead to formation of TiH_2, V_3H_2, NbH, Mg_2FeH_6 or ZrH_2.

Table 3. The energy to remove H atoms and the energy of the Mg atom replaced with other atoms for MgH_2 systems

Mg substitution	One H atom removed/eV	Two H atoms removed/eV	Substitution energy/eV
clean	1.7688	1.9021	–
Ni	0.7456	1.6136	2.1198
Ti	1.6463	2.4763	1.1946
V	1.7062	2.8872	2.0899
Nb	1.6490	1.7606	2.4354
Fe	1.9021	–	0.6912
Zr	1.5592	1.8368	1.3511
Cr	–	–	2.4626
Cu	–	–	2.6967

The energies needed for Ti, V, Nb, Fe, or Zr substitution (as well as Ni itself) at the Mg site are listed in Table 3. It is known that the higher the energy needed for the considered systems, the more difficult the atom substitution is. Hence, in the present work, the substituting elements can be ranked in the following order, according to increasing levels of energy required for substitution: Fe, Ti, Zr, V, Ni, Nb, Cr, Cu (Fig. 7) because the calculated vacancy formation energy is much higher than that (the highest value is 2.6967eV) needed to substitute Ti, V, Nb, Fe, Zr, Cr, Cu at the Mg sites. Hence, the substitution at the Mg site is more energy efficient than the formation of Mg vacancies at lower temperatures. According to the results of Jin et al. [10], neither CuF_2 nor CrF_2 have a significant effect on the dehydrogenation properties of MgH_2 systems, while the substitution of Cr, Cu at the Mg site is the most difficult among all other elements under consideration, thus, we believe that the catalytic effect of CuF_2 and CrF_2 is correlated to its substitution at the Mg site.

The energy costs of removing one or two H atoms from MgH_2 systems are calculated from Eq. (1) (Table 3). Here, Cr and Cu are not considered, due to the difficulty of substituting them at the Mg site. It was found that the energy needed for Ni, Zr, Ti, Nb, or V substitution (not including Fe) at the Mg site is lower than that (1.7688 eV) of pure MgH_2 systems with one H atom removed, which means that elemental substitution improves the dehydrogenation properties of MgH_2 systems and the influence of substitution on the dehydrogenating properties increases in the order Nb, Ni, Ti (Fig. 8).

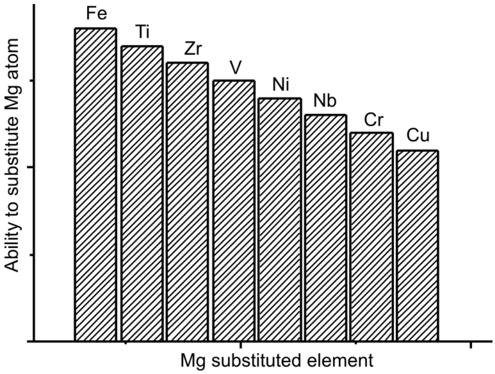

Fig. 7. The order of the Mg atom replaced with another atom

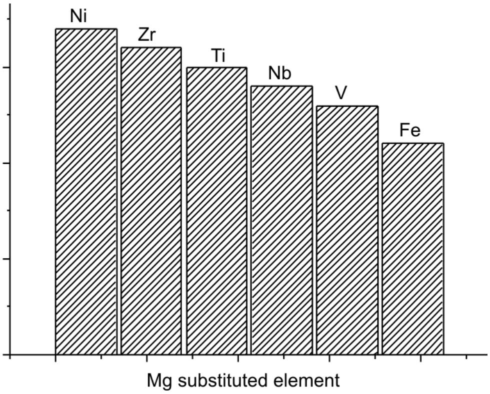

Fig. 8. The calculation order of one Mg atom replaced with other atom in the catalyst effect

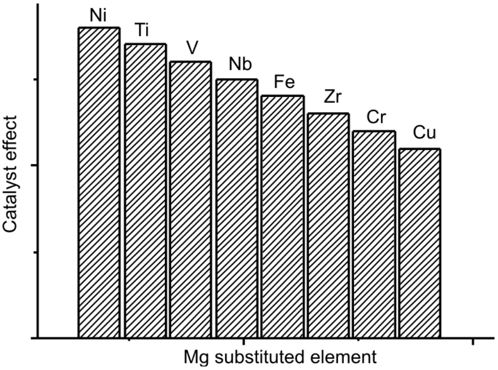

Fig. 9. The experimental order of one Mg atom replaced with another atom in the catalyst effect

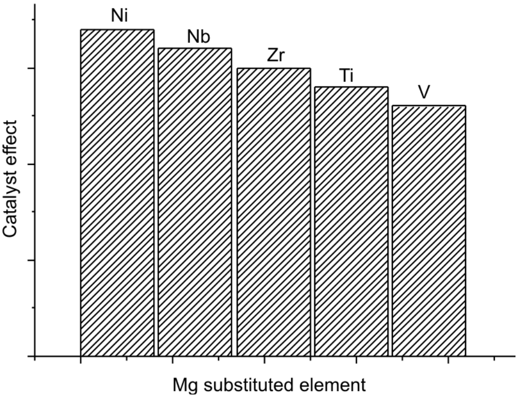

Fig. 10. The calculation order of two Mg atoms replaced with another atom in the catalyst effect

This is in agreement with the experimental results of Jin et al. [10] (Fig. 9). Fe substitution is not considered here, in the case when two H atoms are removed because dehydrogenation of MgH_2 systems is difficult in this case. It was found that the energy needed for Ni, Nb, or Zr substitution (not including Ti and V) at the Mg site is lower than that needed for pure systems (1.9021 eV), which means that Ni, Nb, Zr substitution at the Mg site plays an important role in the dehydrogenation properties of MgH_2 systems. The substituting elements (assuming two H atoms are removed) can be ranked as follows, according to their increasing dehydrogenation efficiencies: Zr, Nb, Ni (Fig. 10). This is also in agreement with the experimental results of Jin et al. [10] (Fig. 9).

In the present work, since MgH_2 systems with removed two H atoms are close to the realistic case in which hydrogen molecule is released, they are investigated in detail as following. Based on Fig. 10, it can be seen that Ni, Nb, or Zr substitution at the Mg site improves the dehydrogenating process for MgH_2 systems, while it is not the case for Fe, Ti, or V substitution, which is not in agreement with the experimental results of Jin et al. [10]. In our group, the characterization of the synthesized duplex $MgH_2 + Mg_2FeH_6$ hydrides mixture has been investigated. We found that the structural stability of the alloying system is reduced when a little iron is dissolved in MgH_2, and further reduced when the iron additions form the compound Mg_2FeH_6. Consequently, the dehydrogenation properties of the corresponding systems are improved [24]. Moreover, based on the calculated energy results for the TiH_2 and $VH_{0.81}$ phase structures, TiH_2/MgH_2 and VH/MgH_2 interfaces were designed. The alloying effects of titanium [25] and vanadium [14] substitution on the dehydrogenating properties of MgH_2 were investigated. It was found that the improved dehydrogenating properties of MgH_2 were caused by titanium or vanadium alloying originates from the increasing of the valence electrons at the Fermi level (E_F) and the decreasing of the HOMO -LUMO gap ($\Delta E_{H\text{–}L}$) after titanium or vanadium alloying. The catalysis effect of titanium or vanadium on the dehydrogenating kinetics of MgH_2 may be attributed to a stronger bonding between the Ti or the V atoms with the H atoms in comparison with the bonding between Mg and H atoms. This stronger bonding leads to easier nucleation of the α-Mg at the TiH_2/MgH_2 or the VH/MgH_2 interface in the MgH_2–Ti or the MgH_2–V systems, compared with the nucleation associated with pure MgH_2 phase. Ti and V both have higher affinity to hydrogen than Mg, and work as a hydrogen pump that chemisorbs hydrogen atoms and transfers them to the TiH_2/MgH_2 or the VH/MgH_2 interface. The nucleation barrier is relatively small. Based on our previous work, the catalytic effect of FeF_2, TiF_3, VF_4 on the dehydrogenation properties of MgH_2 systems (Fig. 9) cannot be caused by Fe, Ti, V substitution at the Mg site. With regard to Fe substitution, the Mg_2FeH_6 compound formed during the milling process acts as the catalyst that improves the dehydrogenation properties of MgH_2 systems [3, 13]. For Ti or V doped systems, the TiH_2/MgH_2 or VH/MgH_2 interfaces help improve the dehydrogenation properties of MgH_2 systems [14]. The effect of FeF_2, TiF_3 and VF_4 on the dehydrogenation properties will be discussed elsewhere. As far as NiF_2, NbF_5 and ZrF_4 are concerned, they are all beneficial for the dehydrogenating kinetics of MgH_2 systems, and the results of our calculations for the improved dehydrogenating kinetics are in agreement with experimental results. If a Ni, Nb, or a Zr atom replaces a Mg atom of a MgH_2 system, the corresponding reactions, namely

$$NiF_2 + 3MgH_2 = MgF_2 + Mg_2NiH_4$$

$$2NbF_5+5MgH_2 = 5MgF_2+2NbH+4H_2$$

or

$$ZrF_4+2MgH_2 = 2MgF_2+ZrH_2$$

that occur during the milling process are accelerated, thus, MgH_2 with the higher stability can be changed into other hydrides such as Mg_2NiH_4, NbH and ZrH_2.

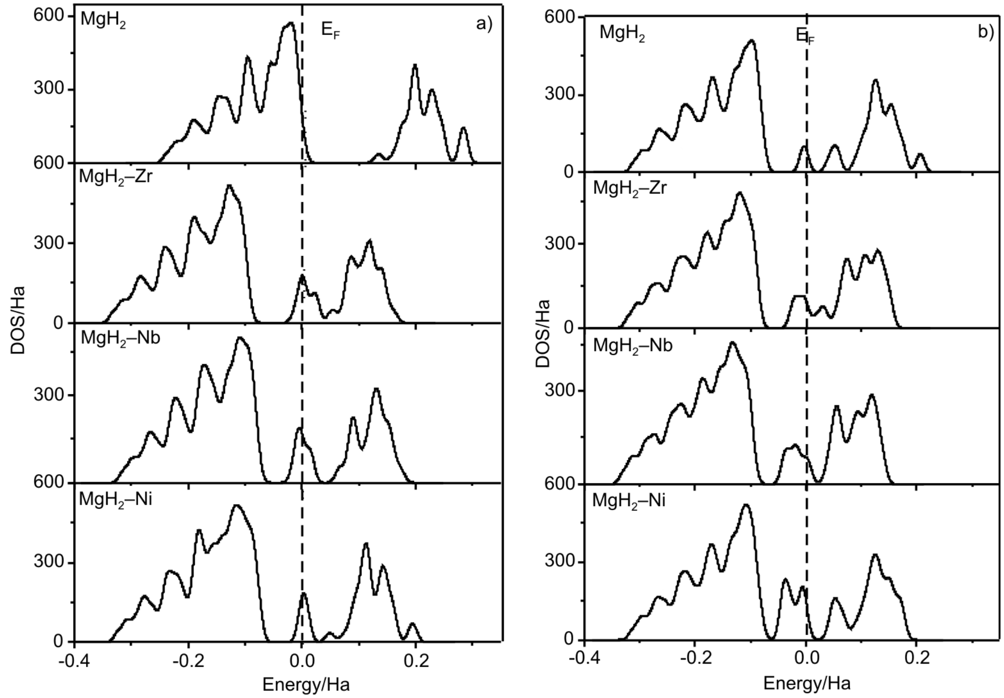

Fig. 11. DOS of MgH_2 systems with Mg atom replaced with another atom (a), and H atoms unchanged (b) two H atoms removed

An analysis was undertaken of the total density of states (DOS) of MgH_2 systems with two H atoms removed and replaced by other atoms, in order to understand the mechanism of the improved dehydrogenation kinetics of MgH_2 systems with metal fluorides (such as NiF_2, NbF_5 ZrF_4, etc.) (Fig. 11). With regard to Mg, with or without Ni, Nb or Zr substitution, it was found that before the dehydrogenation process, the bonding electron numbers below the Fermi energy are 72.14513, 67.13484, 66.13957, 64.10414, which are higher than the corresponding values, (70.11917, 65.06694, 64.07548, 62.07548) for the same systems after the dehydrogenation process. Hence, the bonding strengths/energies for Ni–H, Nb–H and Zr–H are stronger than that for Mg–H. Compared with the density of states (DOS) of MgH_2 systems (Fig. 12), it is found that when a Ni, Nb, or a Zr atom replaces a Mg atom, the valence electron numbers (Fig. 13) lying below the Fermi level in octahedral areas are made of the supercell central atom and the first-nearest and second-nearest H atoms (Fig. 2b) reduce in the order of Ni, Ti, Zr.

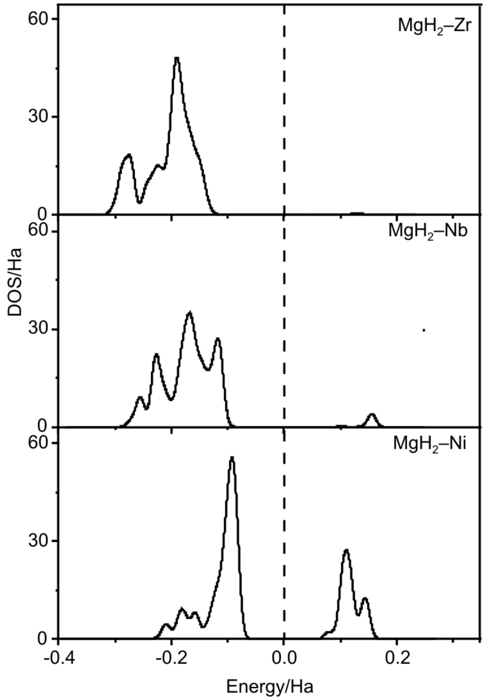

Fig. 12. DOS of octahedral areas in the MgH_2 supercell

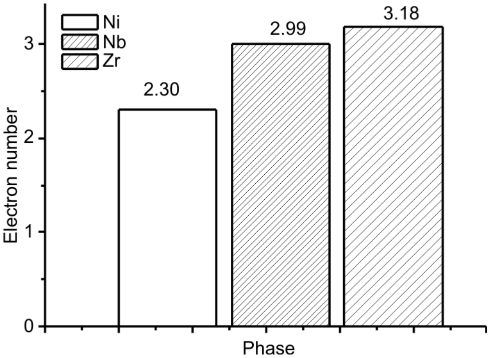

Fig. 13. The number of valence electrons lying below the Fermi level in octahedral areas in the MgH_2 supercell

The higher the bonding electron numbers are, the stronger the charge interactions, and other electron numbers in the low energy range, lying far below the Fermi level, will lead to a more stable structure. Hence, the corresponding structural stability is increased and the dehydrogenation kinetics is less energy-efficient. The density of states (DOS) theory of these MgH_2 systems also provides a very good explanation for the close agreement between the experimental results and the theoretical calculations for predicted improvements to the dehydrogenation kinetics of MgH_2 sytems, if NiF_2, NbF_5, or ZrF_4 are used as catalysts.

4. Conclusions

Density functional theory and the Dmol 4.1 software program were used to calculate the formation energy associated with the replacement of a Mg atom by a different atom, the formation energy of a Mg vacancy, the critical energy needed to remove two H atoms and the electronic structure of MgH_2 systems. The main conclusions are summarized as follows:

The formation energy of a Mg vacancy is higher than that of Fe, Ti, Zr, V, Ni, Nb, Cr, or Cu substitution, which means that the substitution of Fe, Ti, Zr, V, Ni, Nb, Cr, or Cu at the Mg site is more energy efficient than the formation of an Mg vacancy at lower temperatures.

NiF_2, NbF_5, ZrF_4 all improve the dehydrogenation kinetics of MgH_2 systems. The theoretical predictions for these kinetic improvements are in good agreement with the experimental results.

If a Ni, Nb, or a Zr atom replaces a Mg atom of an MgH_2 system, the corresponding reactions that occur during the milling process are accelerated, thus, MgH_2 with the higher stability can be changed into other hydrides such as Mg_2NiH_4, NbH and ZrH_2.

Compared with the density of states (DOS) theory of MgH_2 systems, it was found that when a Ni, Nb, or a Zr atom replaces a Mg atom, the valence electron numbers lying below the Fermi level in octahedral areas are made of the supercell central atom and its first-nearest, second-nearest H atom reduces in the order of Ni, Ti, Zr, meaning the corresponding structural stability is increased and the dehydrogenation kinetics become inferior. The density of states (DOS) theory of these MgH_2 systems also provides a very good explanation for the close agreement between the experimental results and the theoretical calculations for predicted improvements to the dehydrogenation kinetics of MgH_2 sytems, if NiF_2, NbF_5, or ZrF_4 are used as catalysts.

Acknowledgements

The work was supported by the Hunan Provincial Natural Science Foundation of China No. 09JJ6079, the PhD Programs Foundation of Ministry of Education of China No. 200805321032, the Science Fund of State Key Laboratory of Advanced Design and Manufacturing for Vehicle Body No. 60870005.

References

[1] ZALUSKA A., ZALUSKI L., STRÖM-OLSEN J.O., J. Alloys Compd., 288 (1999), 217.
[2] JURCZYK M., SMARDZ L., OKONSKA I., JANKOWSKA E., NOWAK M., SMARDZ K., Int. J. Hydrogen. En., 33 (2008), 374.
[3] SHANG C., X BOUOUDINA M., SONG Y., GUO Z., Int. J. Hydrogen. En., 29 (2004), 73.
[4] HUOT J., HAYAKAWA H., AKIBA E., J. Alloys Compd., 248 (1997), 164.
[5] GENNARI F.C., CASTRO F.J., URRETAVIZCAYA G., MEYER G., J. Alloys Compd., 334 (2002), 277.
[6] LIANG G., HUOT J., BOILY S., VAN NESTE A., SCHULZ R., J. Alloys Compd., 297 (2000), 261.
[7] MANDAL P., DUTTA K., RAMAKISHNA K., SAPRU K., SRIVASTAVA O.N., J. Alloys Compd., 184 (1992), 1.

[8] WANG P., WANG A.M., DING B.Z., HU Z.Q., J Alloys Compd., 334 (2002), 243.

[9] PELLETIER J.F., HUOT J., SUTTON M., SCHULZ R., SANDY A.R., LURIO L.B., MOCHRIE S.G.J., Phys. Rev. B., 63 (2001), 052103.

[10] JIN S.A., SHIM J.H., CHO Y.W., YI K.W., J. Power Sources, 172 (2007), 859.

[11] SONG Y., GUO Z., YANG R., Phys. Rev. B., 69 (2004), 094205.

[12] LI S., JENA P., AHUJA R., Phys. Rev. B., 74 (2006), 132106.

[13] ZHOU D.W., ZHANG J., LIU J.S., PENG P., Chin. Nonferr. Metal., 18 (2008), 2233.

[14] ZHOU D.W., PENG P., LIU J.S., Sci. China Ser. E., 49 (2006), 129.

[15] ZHOU D.W., LIU J.S., PENG P., Sci. China Ser. E., 51 (2008), 979.

[16] PERDEW J.P, BURKE K., ERNZERHOF M., *Phys. Rev. Lett.*, 77 (1996), 3865.

[17] PACK J.D., Phys. Rev. B., 16 (1977), 1748.

[18] DELLY B., J. Chem. Phys., 94 (1991), 7245.

[19] KITTEL C., *Introduction to Solid State Physics*, Wiley, New York, 1986.

[20] HOU Z.F., J. Power Sources, 159 (2006), 111.

[21] FUKAI Y., *The Metal–Hydrogen System*, Springer, Berlin, 1993.

[22] MEDVEDEVA M.I., GORNOSTYREV Y.N., NOVIKOV D.L., MRYASOV O.N., FREEMAN A.J., Acta. Mater., 46 (1998), 3433.

[23] SAHU B.R., Mater. Sci. Eng. B., 49 (1997), 74.

[24] BOGDANOVíC B., BOHMHAMMEL K., CHRIST B., REISER A., SCHLICHITE K., J. Alloys Compd., 282 (1999), 84.

Received 18 August 2009